

SIMULATION STUDY OF THE HIP RESURFACING IMPLANT ORIENTATION

¹HARSHAD AHIRE, ²R.S.TAJANE

¹Bachelor of Engineering, Production Engineering Department, Amrutvahini college of Engineering Sangamner, Savitribai Phule Pune University, Sangamner, Maharashtra , India.

²Associate Professor, Workshop Superintendent, Master of Engineering, Amrutvahini college of Engineering Sangamner, Savitribai Phule Pune University, Sangamner, Maharashtra , India
E-mail: ¹harshadahire@gmail.com

Abstract— The purpose of this paper is to reconstruct a human femur bone by using 2D tomographic slices with hip implant and to perform a static finite element analysis for optimum orientation of hip implant. The 3D human femur was processed using biomedical imaging and editing software packages. The work resulted in three-dimensional solid model can be used in finite element analysis.

Keywords— Biomechanics, Femur, Hip Joint Resurfacing, Finite Element Analysis.

I. INTRODUCTION

The aim of the paper is to demonstrate the process of the patient specific FE analysis of the hip joint implant. For achieving maximum operational life of hip resurfacing surgery. It is necessary to minimize stress induced at the implant and bone interface. In order to do this needs optimization of the orientation and design of implant.

FEA analysis can be used to carry out such patient specific study before Hip resurfacing surgery. The process of FE Analysis starts with the computed tomograms (CT scan) DICOM images of the patient. CT scan data is used for creation of the CAD-model of bone. Then material assignment for the bone derived from the CT scan. Determining the loading conditions under which a normal hip joint will undergo during physical movements of normal human being. The stresses occurring in femur bone at the hip joint due to different implant orientations and implant model parameters is studied.

This workflow would be helpful for applying for similar ortho implants for patient specific implant design.

II. CT SCAN DATA

2.1 Extracting STL from DICOM files

For this study the CT scan data sourced is from the open source online data[1]. There are different tools available for the conversion of the DICOM file data in to STL data. STL data is the faceted representation of the three dimensional file format which can be further used for creation of the cleaner CAD model for analysis. The study was done to evaluate with following tools which can give STL file data.

- 1) *DeVIDE*
- 2) *3D Slicer*

After evaluation 3D Slicer was selected as more user friendly and has better tools to control the segmentation of the bone data.

III. STL FILE GENERATION

3.1 Reading DICOM data

After reading the DICOM file data Volume Rendering module is used for rendering of the 3D region of the scanned area.

With Volume rendering all the region which got scanned like bones, tissues regions all are shown. However to separate out the bone structure out of the full rendered volume we need to use visualize these volume filters. 3D slicer contains filters available as presets.

To separate out the bone structure we can set CT-Bone preset as shown in Figure 1. This will hide all other features of the body scan other than the bone structure. For fine tuning the visible data you can adjust Thresholding level as per the requirement.

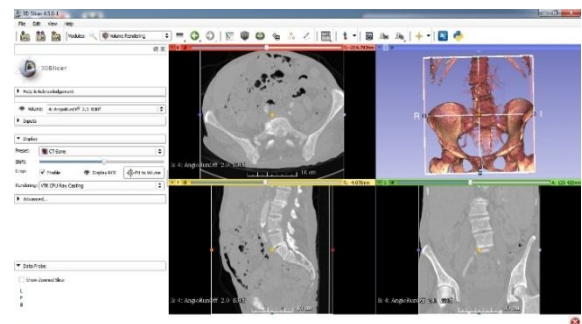


Figure 1 CT Bone Filter

3.2 Region of Interest

The DICOM data that was available was for full abdominal which was oversized relative to the area of interest which is just femur in this study. To restrict the sub volume to the area of interest the Region of Interest (ROI) feature was used.

With use of different views of the ROI was defined and was made sure it covers the area of interest. In this study the region of interest was defined such that it covers left femur. Still it contains some part of the other pelvic bones near the hip joint.

3.3 Crop Volume

The ROI defined in the previous step was defined as the crop volume out of the full DICOM data. This step was essential to reduce the graphics memory requirement of the tool. Also the consecutive steps involved can be only applied to this cropped volume and makes much easier for model handling in graphics. This crop volume is defined as a sub volume of the full rendered data of the earlier volume.

3.4 Creating Label Map

Up to this stage there were two bone regions were fused together the femur and the pelvic bone. Using the Editing module the femur bone was segmented further. In 3D slicer there are pre-defined labels as per body parts which can be tagged to appropriate data. This is also has specified color.

The Editing module contains different region segmentation tools. Which can be categorized as manual and semi-automatic. For segmentation of the femur region Thresholding and manual graphical selection tools were used.

The Thresholding tool requires two input limit values. For cortical bone the lower value is comparatively high around 500 up to a higher value as 1200 was used [2]. Which will give the required cortical bone region only. The region which lies between given two limits starts flashing in graphics. We can pan through all the section views to make sure that the region expected is shown.

At this point the full hip bone and some portion of the pelvic bone are part of the same volume. This gives the region of the cortical bone which is denser and is like the outer shell of bone. The inner cavity represents the cancellous bone (spongy bone).

3.5 Model Creation

Using the Make model effect tool from the Editing module the segmented rendered region of the femur bone was converted to the 3D model.

3.6 Exporting STL file

The model created in the previous step created the cortical bone region of the femur. The inner cavity of this region is the trabecular bone.

IV. BONE GEOMETRY CREATION

4.1 Import STL data

STL data was imported in Ansys Spaceclaim R17. We can also edit and manipulate the STL mesh inside Spaceclaim. Which is required for pre geometry creation operation in most of the cases.

4.2 Removing unwanted STL data

Even though we have the STL data of the required ROI (region of interest) in Slicer. Some nominal cleanup and removal of the unwanted STL clusters was done

manually. Selection tools like box selection or region selection to remove the unwanted STL were used.

4.3 Filling holes

During this removal of the unwanted mesh clusters created the holes in the mesh of the femur bone. Which were filled using the Fill tool.

4.4 Shrink Wrap

The STL model was over detailed mesh which was having some sharp facets and sudden distorted mesh clusters. The Shrinkwrap tool was used to create a single, faceted model that has smooth and uniform facets [3] as shown in **Error! Reference source not found.** and **Error! Reference source not found.**

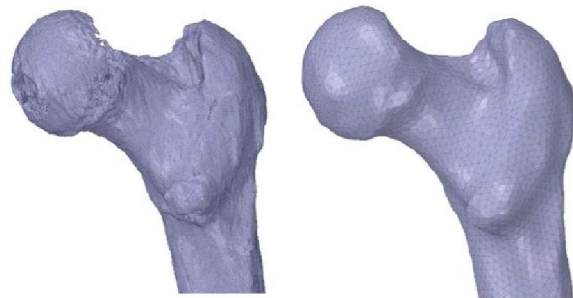


Figure 2 Pre
Shrink wrap STL

Figure 3 Post Shrink
Wrap

4.5 Surface Creation

Creation of skin surfaces is possible in Spaceclaim which requires selection of the mesh nodes which can define a closed loop. Spaceclaim can generate the surface patch by taking reference of underlying facets to create surface path.

With all such patches created we can stitch them together into a closed solid body. This way two solid bodies were created for the cortical region and the trabecular region of the bone. Both the regions possess different material properties. Which requires to separate mesh regions in Ansys Workbench so that two different material bodies are defined. This model was exported in Parasolid file format so that it can be assembled in DesignModeler.

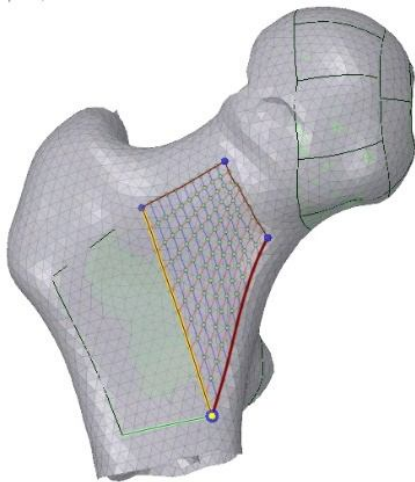


Figure 2 Skin Surface Creation in Spaceclaim

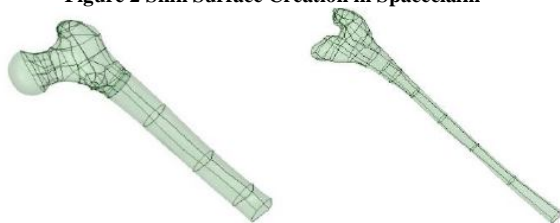


Figure 5 Outer Surface of Cortical Region of Femur.

Figure 6 Outer surface of Cancellous Region of Femur

V. PROSTHETIC MODEL GENERATION

A prosthetic is created based on the size of the bone geometry and then exported in Parasolid format so that can be imported in DesignModeler.

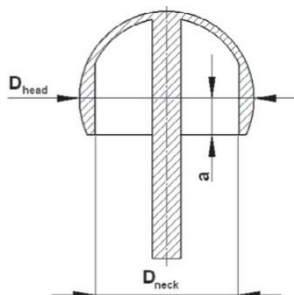


Figure 3 Design Features of Implants

The femoral component was adapted to the anatomical neck diameter 'Dneck' depending on the height 'a' of the spherical cut as shown in Figure 3. The height of the spherical cut is the distance between the center of rotation of the implant and the distal opening of the femoral component[4]. The final implant design details are as shown in the Figure 4

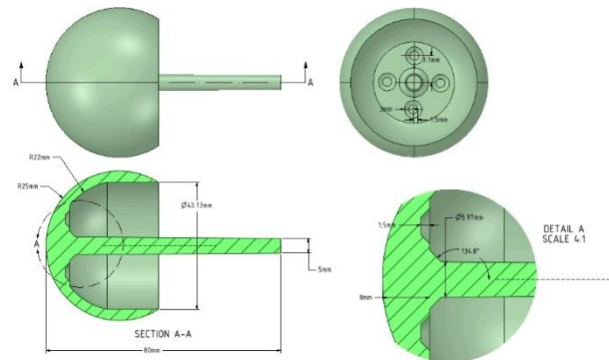


Figure 4 Geometry Details of Femur Implant

VI. GEOMETRY MODELING IN DESIGNMODELER

6.1 Bone and implant Model Alignment

Both the Geometry were imported inside DesignModeler. The implant was oriented such that its stem is aligned with the femur neck axis and is close to the position of the femoral head. To vary the implant alignment with implant neck the geometry operations were added. These alignment angles are two parameters which will be useful for finding optimum implant angle

6.2 Bone Model Editing

To remove the exiting femur head material the slicing operation was done and the extra material from the femoral head was removed.

6.3 Creation of Cement Cavity

To represent the cement portion a cavity between the trimmed femoral end and the implant was filled with the solid cavity region.

6.4 Removing Overlapping Geometry

The overlapping region of the implant stem and the femur was removed. The implant volume was subtracted from bone to create a cavity for the implant stem inside the femur end.

VII. MESH GENERATION

Patch Conforming meshing algorithm was used to create the mesh for the model. Some local refinement regions were defined so that the geometry features are properly captured. The mesh was refined on the following features with following size of mesh.

- 3) Implant stem and top cup
- 4) Bone region around the implant stem
- 5) Cement cavity region

Also to control the max size on the femur the local size was added to geometry. While generating mesh the midside node setting was set as program controlled so that were ever necessary the tool can put higher order cell element can inserted.

VIII. MATERIAL PROPERTIES

The femur model divided into three regions named as thick shaft region as cortical bone, bone marrow inside the cortical and spongy region in proximal and distal end of the bone as trabecular. The linear elastic, orthotropic and heterogeneous material property is assigned for the cortical region and the linear elastic, isotropic and homogeneous material property is assigned for cancellous bone and cortical bone[5]. Material properties for each region are listed in Table 1

Table 1 Material Properties of Femur

Type	Young's Modulus(GPa)	Poission's Ratio
Cancellous Bone	$E_x=126$	$\nu_{xy}=0.055$
	$E_y=19.4$	$\nu_{xz}=0.322$
	$E_z=12.6$	$\nu_{yz}=0.01$
Cortical Bone	$E_x=114.8$	$\nu_{xy}=0.3$
	$E_y=21$	$\nu_{xz}=0.253$
	$\nu_{yz}=1.148$	$\nu_{yz}=0.253$

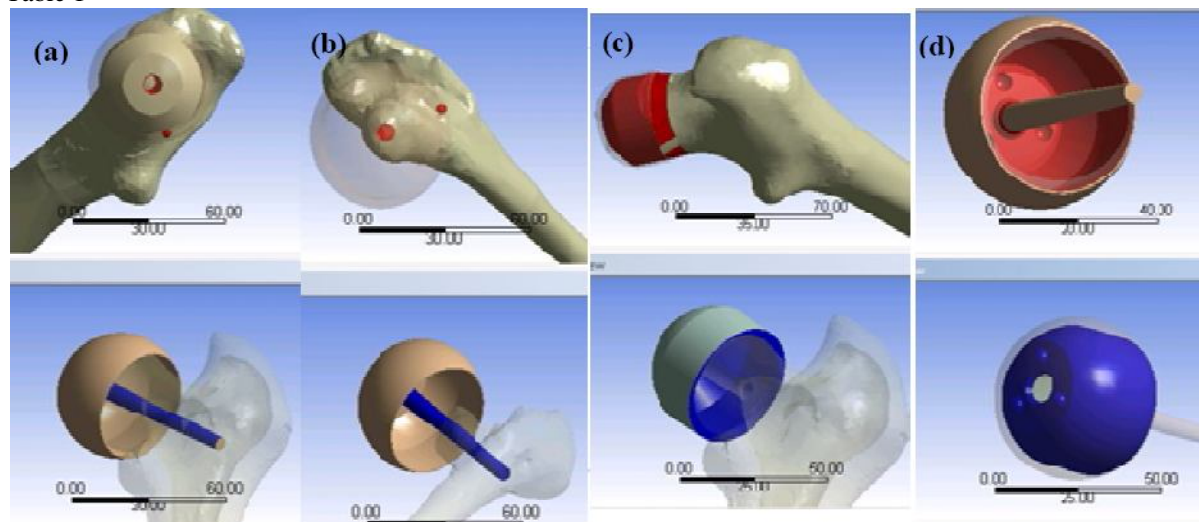
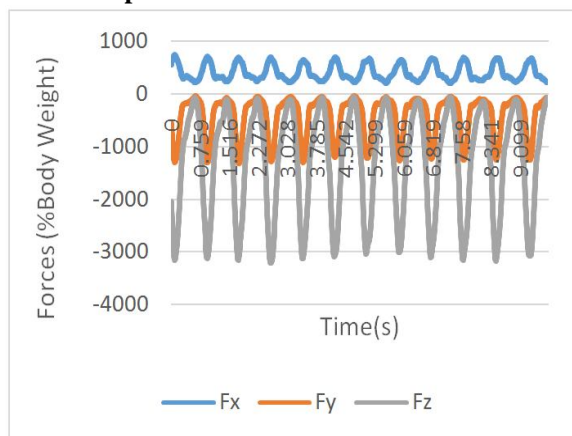


Figure 9 Contact Pairs in Model: (a) Implant – Femur Cortical, (b) Implant – Femur Trabecular, (c) Femur – Cement, (d) Implant – Cement

Chart 1 Hip Joint Forces on Femur



The transfer of the forces bone to implant is primary function of the bone cement. In order to carry out this function bone cement must be compatible with the tissue it contacts and have adequate strength. Since the force transmitted through the hip are high. The widely used material for the cement is that femoral components implanted with poly methylmethacrylate (PMMA)[6].

PMMA has high mechanical strength, high Young's modulus and low elongation at break. It does not shatter on rupture. It is one of the hardest

thermoplastics and is also highly scratch resistant. It exhibits low moisture and water absorbing capacity, due to which products made have good dimensional stability. Both of these characteristics increase as the temperature rises. Material properties for the cement are as mentioned in

Table 2[7].

The ideal material or material combination for Implant should exhibit the following properties[8]:

- A biocompatible chemical composition to avoid adverse tissue reactions
- Excellent resistance to degradation (e.g., corrosion resistance for metals or resistance to biological degradation in polymers)
- Acceptable strength to sustain cyclic loading endured by the joint
- A low modulus to minimize bone resorption.
- High wear resistance to minimize wear debris Generation. The material properties for the Implant are as shown in
- Table 2[9]

Table 2 Cement and Implant Material Properties

Type	Young's Modulus(GPa)	Poisson's Ratio
Cement	2.7	0.3
Implant	210	0.3

IX. MODEL SETUP

9.1 Boundary Conditions

The force is applied on the implant tip. The load acting while jogging on the treadmill with constant speed of 7 km/hr was considered as loading condition for femur. The loading duration is for 2 second of duration as shown in **Error! Reference source not found.** The force data was in the form of components along X, Y and Z axes. Axes X, Y, Z oriented along Medial, Anterior, Superior respectively. The force values shown in **Error! Reference source not found.** are percentage body force which was 815N[10].

The other end of the femur geometry is fixed at the knee joint end.

9.2 Contact Creation

In this model four contacts are defined as following

Error! Reference source not found.

- Implant – Femur Cortical
- Implant – Femur Trabecular
- Femur – Cement
- Implant – Cement

For first three contact pairs there is no separation contact is defined. For the contact between the Implant and the Cement there is no relative motion is expected hence a bonded contact is defined.

9.3 Input and Output Parameters

The most critical region reason for the revision of the hip surgery is aseptic loosening of the implant[11]. Hence to monitor the relative motion between the implant and the bone a sliding distance on the contacts was taken as output.

The input parameters those were defined were for rotation of the implant as shown in.

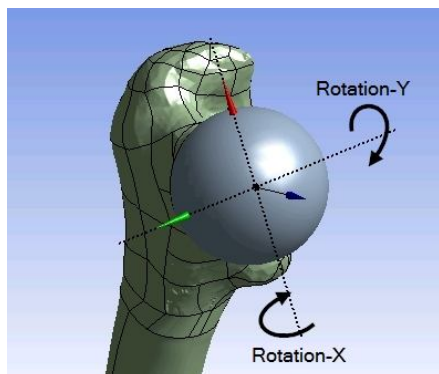


Figure 5 Implant Rotation as Input Parameters

X. RESULTS AND DISCUSSION

10.1 Parametric Simulations

After setting up the model successful initial run was done to make sure the simulation runs without any manual intervention.

The aim of the project is to find optimum orientation of the implant. For this purpose parametric simulations was done using Ansys Design Explorer. Following input and output parameters were defined

- Input Parameters
 - Rotation about X axis
 - Rotation about Y axis
- Output Parameters
 - Equivalent Elastic strain
 - Sliding Distance

Parametric Simulations were performed with nine design points. The values of X and Y angle in range of -2.5° to $+2.5^{\circ}$. The parameter values are as shown in Table 3.

Table 3 Parameter set for Design of Experiments

Rotation-X	Rotation-Y
0	0
-2.5	0
2.5	0
0	-2.5
0	2.5
-2.5	-2.5
2.5	-2.5
-2.5	2.5
2.5	2.5

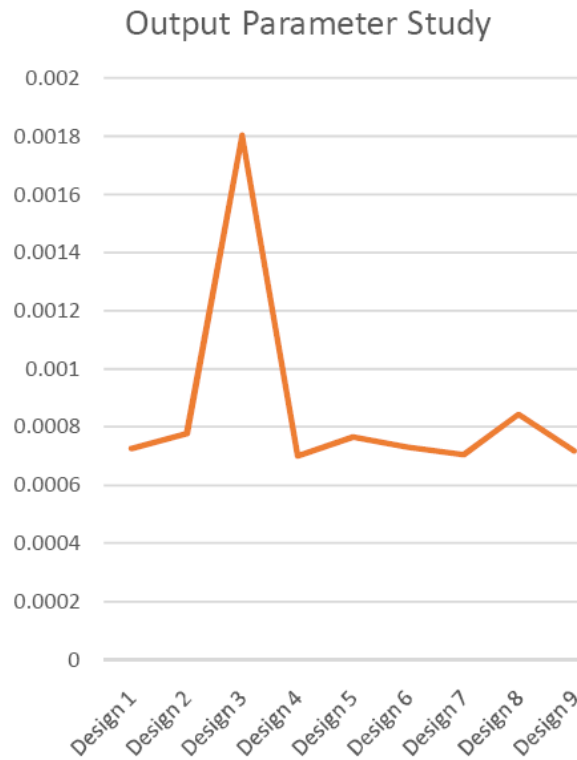
10.2 Optimization

To optimizing the implant orientation. Multiple simulations were run with the input parameters those were shown in

Table 3. With that following sliding distance were found.

Table 4 Maximum Sliding Distance of the Contacts

Design No.	Rotation about X axis (deg.)	Rotation about Y axis (deg.)	Sliding Distance (mm)
1	0	0	0.00072641
2	-2.5	0	0.00077496
3	2.5	0	0.0018029
4	0	-2.5	0.00069936
5	0	2.5	0.00076465
6	-2.5	-2.5	0.00072926
7	2.5	-2.5	0.00070403
8	-2.5	2.5	0.00084401
9	2.5	2.5	0.00071722



As shown in the Table 4 its clear from parameter study that Design 4 which had the X-Rotation of 0 and Y-Rotation -2.5 gives the minimum sliding between the contacts in implant and the bone.

CONCLUSION

The structural behavior was studied of the artificial hip implant using finite element method. The aseptic loosening is one of the most important factor for the revision surgery. With the use of the FEA model and parametric study used to gives clear understanding between the implant and bone. With use of parametric model the optimum implant orientation can help the surgeons to put the implant suitable to specific patients

bone structure and increase the life of the surgery and reduce the revision procedure.

REFERENCES

- [1] "www.osirix-viewer.com," [Online]. Available: <http://www.osirix-viewer.com/datasets/>. [Accessed 01 06 2016].
- [2] D. L. Fat, J. Kennedy, R. Galvin, F. O'Brien, F. Mc Grath and H. Mullett, "The Hounsfield value for cortical bone geometry in the proximal humerus- an in vitro study," *Skeletal Radiology*, vol. 41, no. 5, pp. 557-568, May 2012.
- [3] Ansys Incorporation, Ansys Spaceclaim Help, Ansys Incorporation, 2016.
- [4] D. Kluess, C. Zietz, T. Lindner, W. Mittelmeier, K.-P. Schmitz and R. Bader, "Limited range of motion of hip resurfacing arthroplasty due to unfavorable ratio of prosthetic head size and femoral neck diameter," in *Acta Orthopaedica*, 2008, p. 748.
- [5] M. Verma, N. Bhatnagar, A. Sood, F. Faraz, K. Sharma, G. Venugopal Rao, S. K. Palani and S. Iyer, "Dental implant system". Patent PCT/IN2008/000700, 29 Sep 2010.
- [6] A. Benouis, B. Serier and B. B. B. , "The Mechanical Behavior of Bone Cement in THR in the Presence of Cavities," *Engineering, Technology & Applied Science Research*, vol. 4, no. 3, pp. 625-630, 2014.
- [7] Technical University of Gabrovo, Tampere University of Technology and Institute of Materials Science, "<http://webhotel2.tut.fi>," [Online]. Available: http://webhotel2.tut.fi/projects/caeds/tekstit/plastics/plastic_s_PMMA.pdf. [Accessed 12 Jun 2016].
- [8] D. S. Deb, "Part-III -Mechanical Properties of Bone Cement," in *Orthopedic Bone Cement*, Woodhead Publishing in Materials, p. 233.
- [9] Y. S. A. Jabbari, "Physico-mechanical properties and prosthodontic applications of Co-Cr dental alloys: a review of the literature," *Journal of Advance Prosthodontics*, vol. 6, no. 2, p. 138-145, 2014 Apr.
- [10] "www.orthoload.com," Julius Wolff Institute of the Charité in Berlin, [Online]. Available: <http://orthoload.com/database/>. [Accessed 10 June 2016].
- [11] D. Kluess, J. Wieding, R. Souffrant, W. Mittelmeier and R. Bader, "Finite Element Analysis in Orthopaedic Biomechanics," in *Finite Element Analysis*, D. Moratal, Ed., Rostock, Germany, Sciyo, 2010, p. 159.
- [12] "Chapter 1 Overview of Biomaterials and Their Use in Medical Devices," in *Handbook of Materials for Medical Devices*, ASM International, 2003, p. 1.
- [13] E. T. Davis, M. Olsen, R. Zdero, J. P. Waddell and E. H. Schemitsch, "The Journal of Bone and Joint Surgery (Br)," *Femoral neck fracture following hip resurfacing*, vol. 90, no. B, pp. 1522-7, 2008.

★ ★ ★